

Journal of Materials Chemistry A

Accepted Manuscript



This is an *Accepted Manuscript*, which has been through the Royal Society of Chemistry peer review process and has been accepted for publication.

Accepted Manuscripts are published online shortly after acceptance, before technical editing, formatting and proof reading. Using this free service, authors can make their results available to the community, in citable form, before we publish the edited article. We will replace this *Accepted Manuscript* with the edited and formatted *Advance Article* as soon as it is available.

You can find more information about *Accepted Manuscripts* in the [Information for Authors](#).

Please note that technical editing may introduce minor changes to the text and/or graphics, which may alter content. The journal's standard [Terms & Conditions](#) and the [Ethical guidelines](#) still apply. In no event shall the Royal Society of Chemistry be held responsible for any errors or omissions in this *Accepted Manuscript* or any consequences arising from the use of any information it contains.

Supercapacitive Properties of Coiled Carbon Nanotubes Directly Grown on Nickel Nanowires

F. Hekmat^a, B. Sohrabi^{*, a}, M. S. Rahmanifar^b, M. R. Vaezi^c

Proofs and Correspondence to:

Dr. Beheshteh Sohrabi

E-mail: sohrabi_b@yahoo.com, sohrabi_b@iust.ac.ir

Fax: +98-2177491204

Supercapacitive Properties of Coiled Carbon Nanotubes Directly Grown on Nickel Nanowires

F. Hekmat^a, B. Sohrabi^{*, a}, M. S. Rahmanifar^b, M. R. Vaezi^c

^a Department of Chemistry, Surface Chemistry Research Laboratory, Iran University of Science and Technology, P.O. Box 16846-13114, Tehran, Iran.

^b Faculty of basic science, Shahed University, Tehran, Iran.

^c Advanced Materials Research Center, Materials and Energy Research Center, Karaj, Iran.

Abstract

In this paper, Coiled carbon nanotubes (CNTs) have been grown directly on an anodized aluminum oxide (AAO) template by using catalytic chemical vapor deposition (CVD). The nanochannels of the AAO template which is covered from one side with conducting Au layer were filled by using Catalytic Ni nanowires (Ni-NWs). Scanning electron microscopy (SEM/EDX) and Raman spectroscopy were used to prove the formation of coiled CNTs on Ni-NWs. Cyclic voltammetry, galvanostatic charge-discharge, and impedance spectroscopy were used to investigate the capacitive behavior of coiled CNT/Ni-NW. Electrochemical analysis reveal that the coiled CNT/NW porous structured materials as electrodes for supercapacitors exhibit a high specific capacitance (202 F g^{-1} at a current density of 10 A g^{-1}) as well as excellent cycle stability which can retain more than 92% of its initial response after 6000 cycles. On the other hand as prepared coiled CNT/Ni-NW electrode worked at a wide potential window (2.1 V) in $1 \text{ M Na}_2\text{SO}_4$ aqueous solution at room temperature. Combining the specific capacitance with large electrochemical window insure the superior energy and power densities nanostructure

electrodes which would be useful to improving performances for new energy storage technologies.

Keywords: Coiled Carbon Nanotubes, Chemical Vapor Deposition, Anodic Aluminum Oxide, Ni Nanowires, Supercapacitors.

1. Introduction

In recent years, Electric double layer capacitors (EDLCs) which also named as supercapacitors are expected to play an important role as a charge-storage system which store the energy within the electrochemical double layer at the electrode/electrolyte interface.¹ EDLCs are able to store greater amounts of energy than the traditional dielectric capacitors, furthermore they can be charged or discharged quickly, so they have ability to deliver more power than the batteries.²⁻⁴ Consequently, EDLCs fill the gap between batteries and traditional capacitors which was previously vacant.⁵ Supercapacitors have only very recently being developed as energy storage systems for wide range of applications requiring continuous current pulses with high power density including portable devices, hybrid vehicles, digital communication systems, medical electronics, military devices, and back-up systems.^{6,7} Since the charge storage in EDLCs was happened on the electrode surface, their performance tightly depends on optimizing of electrode materials.

The favorable chemical and physical properties of carbon materials, such as large specific surface area and relatively high electrical conductivity which are respectively guarantee the appropriate energy and power densities, makes them good option for the electrodes of

supercapacitor.^{8,9} Among different types of carbon materials, owing to their unique properties of high electrical conductivity, high surface area, high charge transport capability, high mesoporosity, high electrochemical stability, and high electrolyte accessibility, CNTs attract much attention for developing high-performance supercapacitors.¹⁰⁻¹²

Shortly after their discovery by Iijima in 1991,¹³ different shapes of CNTs have been reported.¹⁴ Since the behavior of CNTs strongly depends on their structures, so several researches have been done to develop new design of CNTs in order to make CNT materials more suitable for variety of applications, such as improving the electrochemical performance, safety, and lifetime of CNT electrode materials for supercapacitors.¹⁰

In the early 1990s, coiled CNTs with unique molecular and electronic properties were experimentally reported.^{15, 16} This kind of CNTs is formed by creation of paired pentagon and heptagon carbon rings which arrange themselves periodically within the CNT network basically formed from hexagonal rings.¹⁴ Motojima et al. reported that coiled carbon fibers were obtained on a graphite substrate by the catalytic pyrolysis of acetylene containing a small amount of thiophene impurities using Ni particles as catalyst.¹⁶ Among different methods for growing CNTs,¹⁷ due to their advantages, such as simplicity of the growth, cost effective, ability to grow CNTs on a wide range of substrates, and being able to grow a large scale of high purity CNTs,^{18,}¹⁹ CVD-based methods attracted much attention for finding the optimal condition to obtain coiled carbon nanotubes on a desired substrate. In 1994, Amelinkx et al. investigated the role of cobalt as a catalyst and acetylene as a carbon source in growing well-graphitized and extremely thin coiled nanotubes.²⁰ Iwanaga group reported that a small amount of impurity in hydrocarbon source plays an important role as an activation agent for the growth of the coiled carbon whiskers.²¹ Pradhan et al. gave a detailed description about the role of pyrolysis temperature and catalysts in

fabrication procedure for coiled CNTs by using a thermal CVD process.²² Bai used catalytic decomposition of acetylene on AAO template with aid of Ni as catalyst to obtain very pure coiled carbon nanostructures.²³ Coiled carbon nanotubes were grown through methane decomposition over Co/Al₂O₃ under an adjusted pyrolysis temperature, by Takenaka and coworkers.²⁴

Akagi et al. demonstrated that unlike the straight CNTs which exhibit only metallic or semi conductive electrical conduction, the coiled CNTs can show even semi metallic characteristics, which could not be manifested in straight CNTs.²⁵ The sharp peak of the corresponding densities of the states (DOS) of coiled CNTs at the Fermi level indicated that the coiled CNTs could be a valuable superconductor material which can be used in wide range of applications such as EDLCs.²⁵

Based on previous researches, it is expected that the coiled CNTs/Ni-NWs will have impressive electrochemical performance in supercapacitors, so to prove this hypothesis, the capacitive properties of as grown coiled CNTs based electrodes were investigated in this paper.

2. Experimental

2.1. Chemicals

High-purity aluminum foil (99.9995%, Merck, Germany), Perchloric acid (60%, Merck, Germany), ethanol(96%, Jonoob, Iran), oxalic acid 2-hydrate (99%, Panreac Quimica SA, E.U.), Chromic anhydride (KANTO Chemical Co. INC, Japan), phosphoric acid (85%, Merck, Germany), copper sulfate (Merck, Germany), chloridric acid (36%, Merck, Germany), hexahydratenickel sulfat (Merck, Germany), heptahydratenickel chloride (Merck, Germany), boric acid (Merck, Germany), sulphuric acid (96%, Merck, Germany), and sodium sulfate

(Merck, Germany) were used as received. Finally, double ionized water was obtained from an OES water purification system (Oklahoma, USA).

2.2. Equipments

DC power suppliers (MP6003, Megatek, Germany) were used in order to apply electric field in preparation of AAO template and also electrochemical deposition of Ni-NWs in the nanopores of AAO substrate. The samples investigation were done by using scanning electron microscopy (TESCAN, VEGA, Czech Republic), field-emission scanning electron microscope (TESCAN, Mira II LMU, Czech Republic) which was equipped with an energy-dispersive X-ray spectroscopy (EDX) probe, X-ray power diffraction (XRD) (X'Pert Pro MPD, PANalytical, using Cu K α Radiation), and Raman spectroscopy (BRUKER, SENTERRA, Germany). Thermal gravimetric analysis (TGA) was performed with a Thermogravimetric Analyser (METTLER TOLEDO TGA/SDTA 851, Switzerland). The measurements were carried out in the range 25–1100 °C, with a 10 °C min⁻¹ heating rate under flowing 30 cm³ min⁻¹ of air. The specific surface area was measured by Brunauer–Emmett–Teller (BET) method at 77 K in N₂ atmosphere using surface area analyzer (PHSCHINA, PHS-1020, China). Different electrochemical techniques were used to characterize the capacitive performance, and internal resistance of prepared electrodes. Cyclic voltammetry (CV) measurements were conducted on Electroanalyzer system SAMA 500 (Iran), in a potential range between -1.2 and +1 V vs. Ag/AgCl reference electrode at scan rates of 10-100 mV s⁻¹. The galvanostatic charge-discharge measurements were performed on a Cell tester Kimiastat 126 (Iran), at different current densities within the same voltage window for the CV analysis, and the cyclic stability was characterized up to 6000 cycles. Electrochemical impedance spectroscopy (EIS) was carried out to prove the capacitive performance at open circuit potential,⁴ by an Auto lab PGSTATE 30 controlled by computer and

Nova 1.7 software, applying an alternating current in the frequency range from 100 kHz to 0.1 Hz. All of the electrochemical tests were carried out in 1M Na₂SO₄ aqueous solution at room temperature in a three electrodes configuration using a saturated Ag/AgCl electrode as the reference electrode and a graphite counter electrode.

2.3. Electrode preparation

2.3.1. Preparation of AAO template

The preparation steps for coiled CNTs/Ni-NWs electrodes is illustrated in Fig. 1. First, a 30mm×30mm×0.3mm aluminum sheet was degreased in acetone ultrasound and rinsed in an ethanol solution, followed by annealing at 500°C for 5 h.²⁶ The annealed sample was electropolished in a 1:4 volume mixture of perchloric acid (60wt %) and ethanol (96wt %) at 3°C, and constant DC voltage of 20 V for 1 min were applied to obtain mirror finish, before anodizing (Fig. 1a). The two-step anodizing was chosen to prepare an ordered porous AAO template. The first anodizing was carried out under a constant voltage of 45V DC in a 0.3 M oxalic acid solution at 5°C for 20 h. The AAO film was chemically etched in a mixture of chromic acid (1.8 wt%) and phosphoric acid (6wt%) at 75°C for 3 h, then the second anodizing process was done for 4 h, under the same conditions as the first anodization process, which resulted in formation of a highly ordered porous AAO template with a pore depth of about 6.5 μm.^{26, 27} In order to facilitate the uniform electrodeposition of nickel nanoparticles in growing Ni-NWs, the voltage was dropped from 45 to 14V at the rate of 0.5 Vmin⁻¹, which was done immediately at the end of the second anodization. Because the thickness of the barrier layer is

proportional to applied voltage, the barrier layer was almost completely removed when the voltage reached 14 V.²⁸⁻³⁰

After elimination of the barrier layer, the remaining Al substrate was partially removed in a saturated copper sulfate (CuSO_4) aqueous solution in chloridric acid (HCl) at room temperature.³¹ Finally, the resulting AAO template was immersed in a 1M aqueous phosphoric acid solution at a room temperature for 40 min, to eliminate the barrier layer on the bottom side, and simultaneously widen the pores (Fig. 1b).²⁹ One side of AAO membrane was sputtered with a layer of Au as a work electrode. Ni-NWs were used as catalyst for CNT growing were electrochemically deposited in the pores of AAO template by a three-electrode electrochemical system, from an aqueous solution of 330g L^{-1} $\text{NiSO}_4 \cdot 6\text{H}_2\text{O}$, 45 g L^{-1} $\text{NiCl}_2 \cdot 6\text{H}_2\text{O}$, and 35 g L^{-1} H_3BO_3 solution, called Watt bath at 23°C .³¹ To get the better results in electrodeposition of Ni catalysts in the bottom of pores, pH value of the electrolyte was adjusted to about 2.0 with 0.1 M H_2SO_4 solution.³¹ The electrochemical deposition of Ni-NWs was performed by using AAO template, which sputtered with a layer of Au, as working electrode, platinum as counter electrode, and Ag/AgCl as reference electrode, and all of the potentials refer to the reference electrode. The deposition rate is about 8.4 nm s^{-1} , so we can easily control the length of Ni-NWs properly selecting the electroplating time.³² Ni-NWs deposited at 1.0 V for 20 min, to fulfill the nanoholes of AAO template (Fig. 1c).

2.3.2. Growing coiled CNTs

The coiled CNTs were grown by a thermal-CVD system using the Ni-NWs as catalyst, mixture of hydrogen and Argon as carrier gas, and the acetylene as reaction gas.

After depositing the Ni-NWs in the nanoholes of AAO template, the substrate was cleaned in acetone and rinsed in an ethanol solution. The AAO templates were placed into a quartz reaction

tube in high temperature tube furnace. Carrier gas flowed into the quartz tube while the furnace was heated. Ni nanoparticles were reduced in a gas mixture of 10% H₂ and 90% Ar at 500°C for 1h. CNTs were then grown by catalytic pyrolysis of 10% C₂H₂ and 20% H₂ in an Ar carrier gas at a total flow rate of 150 sccm for 60 min at 650°C (Fig. 1d). After dissolving the AAO template with aid of 0.1M KOH (Fig. 1e), the capacitive behavior of as prepared electrodes were measured.

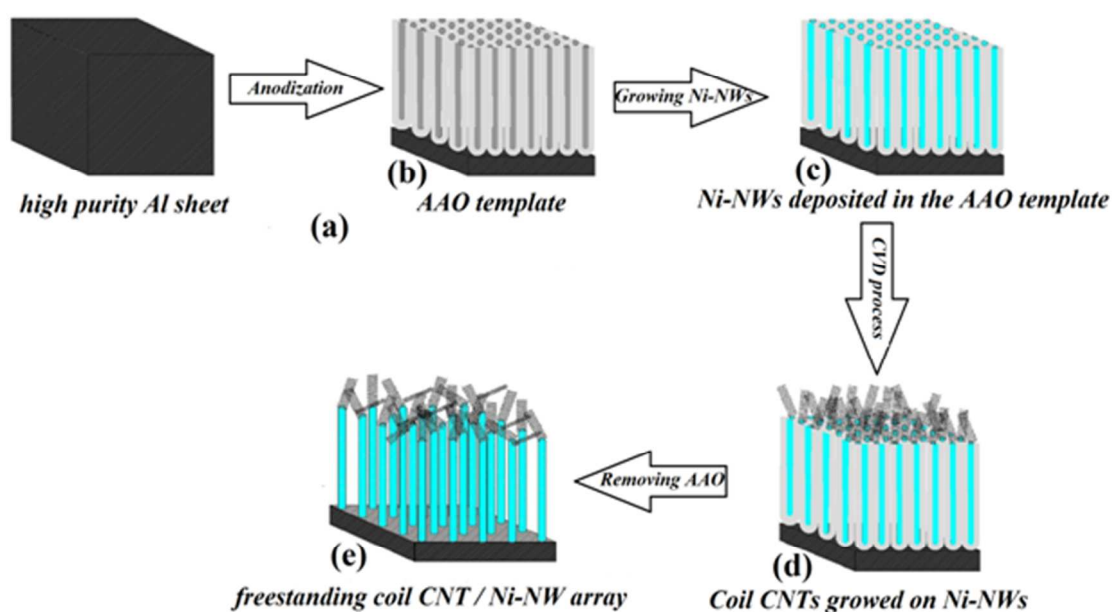


Fig. 1. A schematic illustration of the fabrication processes of the coil CNT/Ni-NWs electrode.

3. Results and discussion

3.1. Structure characterization

Fig. 2a is a plane image of the AAO template taken by FE-SEM showing a porous Al₂O₃ layer with straight and uniform pores after a two-step anodizing, and pores widening treatment. The average cylindrical pore diameter and pore density of the prepared templates were 50±5 nm and

2×10^{10} pores cm^{-2} , respectively. Fig. 2b shows the morphology of a treated AAO template taken after growth of Ni-NWs in the pores, showing the Ni-NWs deposited uniformly to fill the pores. Fig. 2c illustrates the cross sectional view of AAO template after deposition of coiled CNTs. The inset is a high magnification image of coiled CNT which were covered the surface of the electrode. Fig. S1† shows the EDX analysis of the region which remarked in Fig. 2c. The EDX results are trustworthy indicates the deposition of CNTs on the AAO template which pores were filled by Ni nanowires.

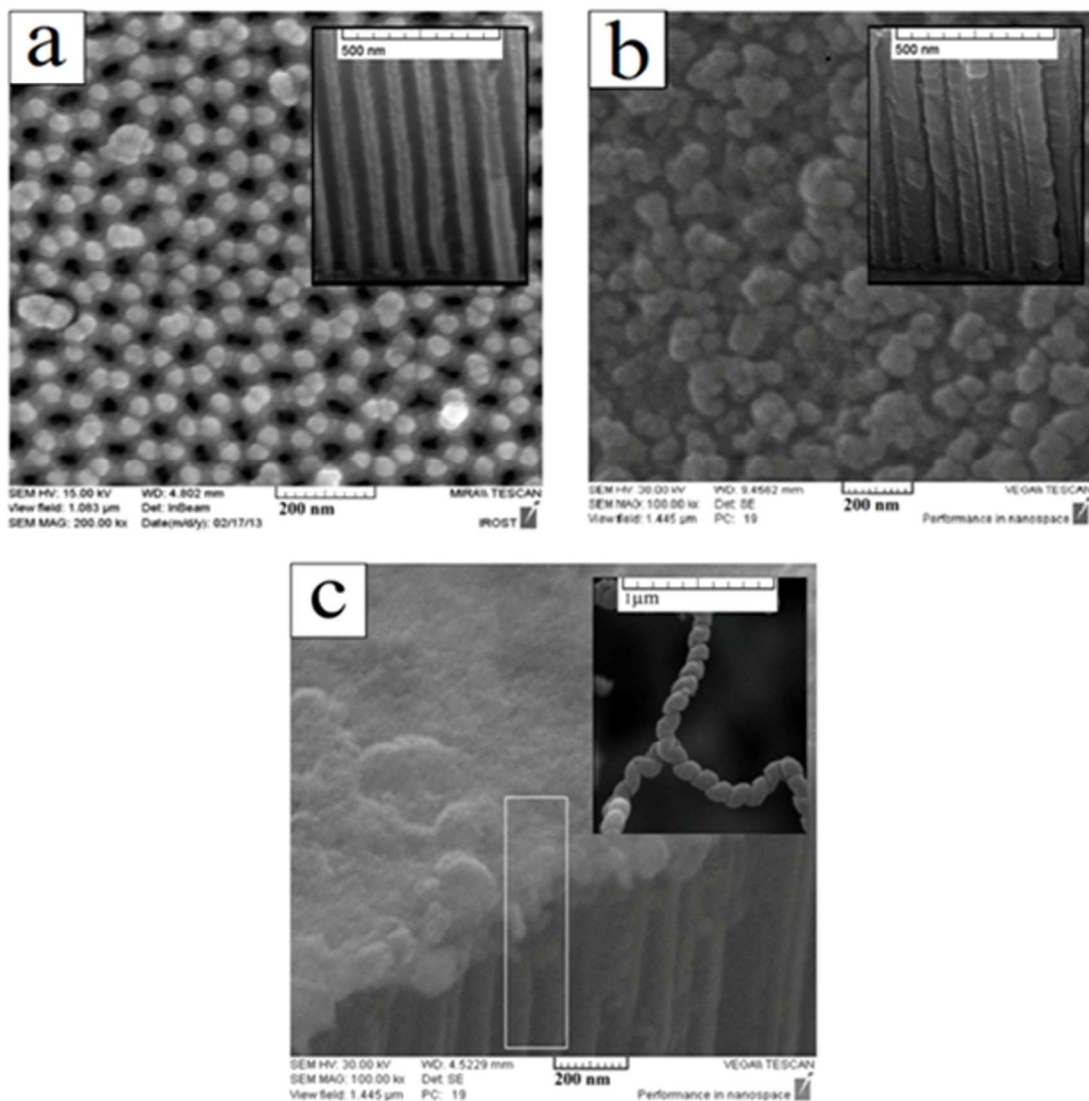


Fig. 2. Plane view of porous AAO template (a) before and (b) after electrochemical deposition of Ni-NWs, insets: cross sectional view of AAO template before and after Ni-NWs deposition, respectively. (c) Cross sectional image of template after growing coiled CNTs by a thermal-CVD system using the Ni-NWs as catalyst, inset: High magnification of coiled CNTs grown on top of the substrate.

The XRD pattern of a coiled CNT/Ni-NW electrode is presented in Fig. 3, where the characteristic peaks of the CNT are observed. The strong diffraction peak at 2θ value of 26.02° corresponding to (002) crystal plane indicates the formation of CNT (JCDPS, card no 00-025-

0284). No other peaks which refer to highly crystalline CNTs can be observed in the spectra which indicate that the presence of disorders or defects in the graphite structure of the CNTs. The strong peaks at 2θ values of 44.47° , 51.83° , and 76.33° corresponding to (111), (200), and (220) crystal planes indicate the formation of cubic crystalline nickel (JCDPS, card no 01-070-1849). Moreover, according to observation of the strong peaks at 38.54° , 43.41° , 65.08° , and 78.17° corresponding to (111), (200), (220), and (311) crystal planes we can guarantee that the sample is containing Al (JCDPS, card no 01-089-2769), which is used as current collector in as prepared electrode. Fig. S2† displays the XRD pattern of the coiled CNT/Ni-NW electrode before removing the AAO. We can clearly see that all the diffraction peaks indicate the formation of CNTs on AAO/Al based template in presence of crystalline Ni.

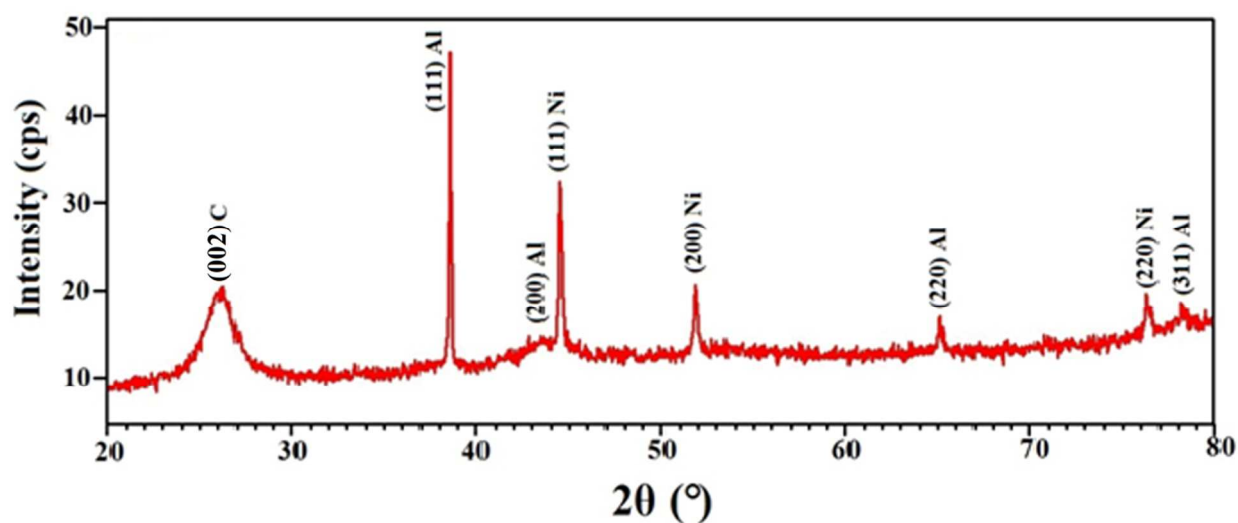


Fig. 3. XRD pattern of coiled CNT/ Ni-NW based electrode.

Raman spectroscopy is a method which is commonly used for the structure characterization of different types of carbon materials.³³ Raman spectroscopy analysis of coiled CNTs is shown in Fig.4. The band at 1580 cm^{-1} , which is called G-band, originates from in-plane vibration movement of carbon atoms in the CNTs, and the D-band at 1286 cm^{-1} is represents the degree of

disorder in the graphite structure or the number of defects in the CNTs.^{31,34-37} The I_D/I_G ratio of the as-grown coiled CNTs is 1.45 which indicates the presence of pentagon-heptagon atomic rings within the hexagonal carbon network, which are known as defects.⁷

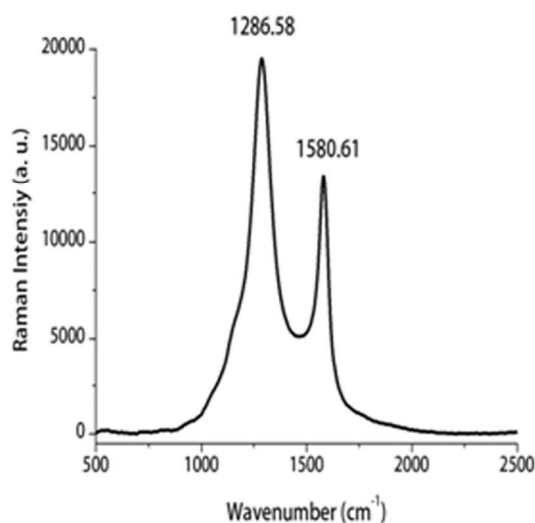


Fig. 4. Raman spectrum of the coiled CNTs shown in the inset of Fig. 2c.

Thermogravimetric analysis (TGA) was performed to precisely determine the coiled CNTs content in the coiled CNT/Ni-NW electrode. Fig. 5 shows the TGA plots of template, before and after growing coiled CNTs. For both samples, the same trend of degradation pattern which can refer to Ni/Al based substrate was shown. Based on comparing TGA results of the template before and after deposition of coiled CNTs, the coiled CNT began to oxidize at $\sim 550^\circ\text{C}$, and a small increasing in weight which is started from $\sim 100^\circ\text{C}$, probably attributed to the partial oxidation of metallic components in the sample. It can also be seen from Fig. 5 that the weight loss of the coiled CNT content in the as prepared electrode is approximately 20 wt%.

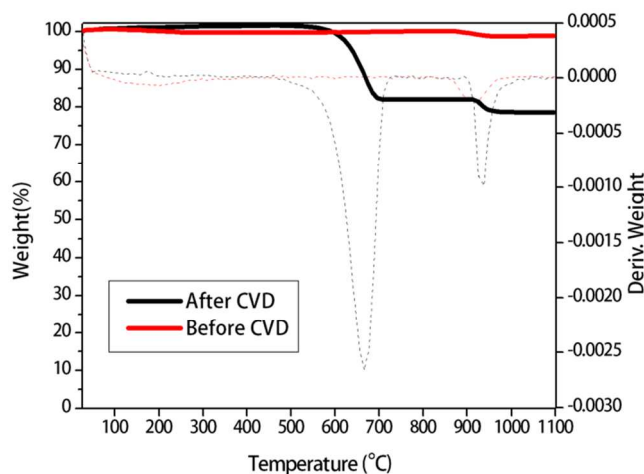


Fig. 5. TGA profiles of template before and after deposition of coiled CNT.

Fig. 6 represents the nitrogen adsorption/desorption isotherms of the free standing coiled CNTs/Ni-NWs. The specific surface area is $\sim 170 \text{ m}^2 \text{ g}^{-1}$. Furthermore, the sample exhibit type IV nitrogen adsorption–desorption isotherms, indicating the presence of mesopores. The inset shows the pore size distribution plot according to the BJH method. Based on the results, the average pore diameter is 2.61 nm. Combination of the large specific surface area and suitable pore size distribution guarantee a reasonable electrochemical performance of coiled CNT/Ni-NW based electrodes³⁸.

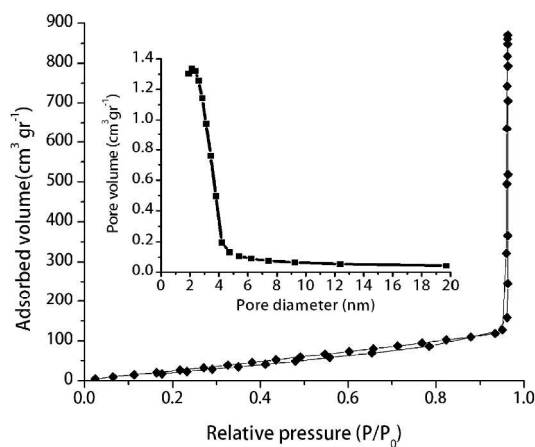


Fig. 6. Nitrogen adsorption–desorption isotherms (with the BJH pore size distributions plots in the insets.) measured at 77 K for coiled CNT/ Ni NWs.

3.2. Electrochemical performance of the coiled CNT/Ni-NW electrode

Cyclic voltammetry is useful as a quick screening procedure to identify potential capacitor materials.³⁹ The cyclic voltammetry method is used for determination of potential window of active material. Fig. S3† shows the cyclic voltammetric responses of the CNT/Ni NWs at different working potential windows at a scan rate of 100 mV s^{-1} in $1 \text{ M Na}_2\text{SO}_4$ electrolyte, which is in good agreement with previous reports about the wide potential window of carbon based materials in a neutral medium as electrolyte.⁴⁰⁻⁴² The observed quasi-rectangular shape of the CV curves (Fig. S3†) suggests that the CNT/Ni NW supercapacitor exhibits capacitive behavior over a large working potential window.

Fig. 7a presents the cyclic voltammograms of as prepared coiled CNT/Ni-NW electrode in the aqueous solution of $1 \text{ M Na}_2\text{SO}_4$ at different scan rates in the potential range of -1.2 to $+1 \text{ V}$. The CV shapes of the prepared electrode are nearly rectangular, indicating a relatively low resistance, which attributed to homogeneously coating current collector with coiled CNTs, without binder, so it makes them valuable candidates for the electrodes of supercapacitor which possess superior responsibility in high current densities. Fig. 7a represents a mirror-image which proves the reversibility of as fabricated electrode reaction.⁷ Due to the absence of prominent peaks within the potential window, we can claim that the resultant capacitance is only obtained from double layer capacitance without any pseudocapacitive reactions which guarantees the long cycle life of this kind of electrode materials. Moreover, it could be observed that the CV curves of the prepared electrode was kept with increasing the scan rate from 20 mVs^{-1} to 100 mV s^{-1} , which could be attributed to the unique porous structure of the coiled CNT/Ni-NW electrode, which enhanced the accessibility for electrolyte ion transport.⁴³ Combination of the results which obtained from cyclic voltammograms insures the good capacitive performance of coiled

CNT/Ni-NW based electrodes during the high discharge current densities. The specific capacitance was calculated from the corresponding CVs (Fig. 7a) according to the following equation:

$$C_{sp} = \frac{I}{\left(\frac{dV}{dt}\right)}$$

where C_{sp} is the specific capacitance ($F\ g^{-1}$), I is the current density ($A\ g^{-1}$), and $\frac{dV}{dt}$ is the scan rate ($V\ s^{-1}$). As shown in Fig. 7b, the capacitance of prepared electrode decreased slightly upon increasing the scan rate, from $275\ F\ g^{-1}$ in $20\ mV\ s^{-1}$ to $213.5\ F\ g^{-1}$ in $100\ mV\ s^{-1}$, which can be attributed to diffusion limitations of the electrolyte in the pores of the electrode material, caused by increasing of the resistance which occurred simultaneously with increasing of scan rate.⁴³

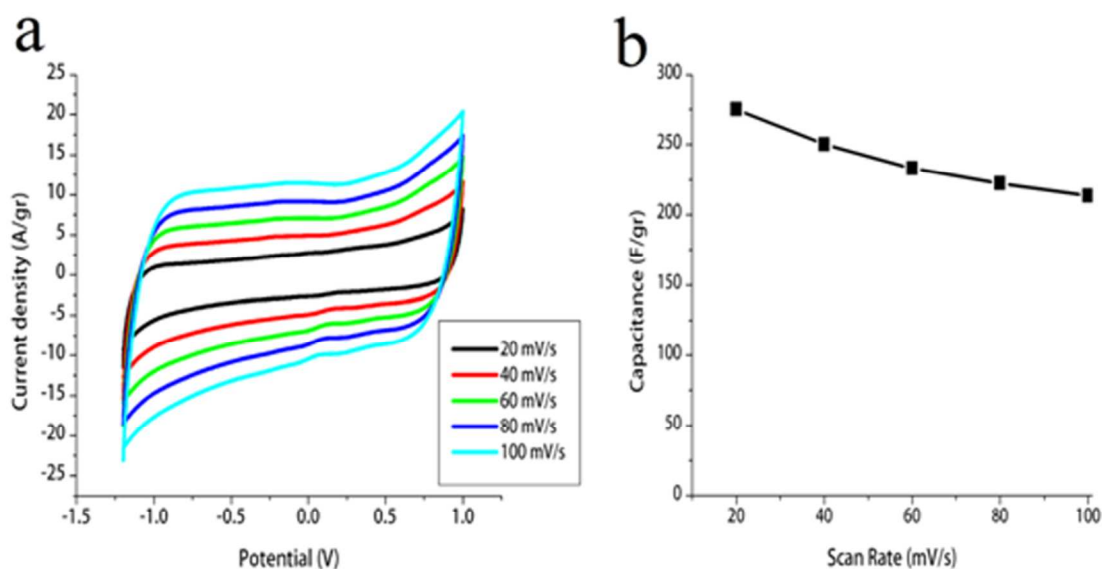


Fig. 7. (a) Nearly rectangular cyclic voltammograms of the coiled CNT/Ni-NW electrode measured in 1.0 M Na₂SO₄ at the scan rates increasing from $20\ mV\ s^{-1}$ to $100\ mV\ s^{-1}$, and (b) the dependence of the capacitance of the electrode on the applied scan rates.

Galvanostatic charge-discharge experiments were performed to further capacitive performance investigation of the coiled CNT/Ni-NWs electrodes, with the voltage window of 2.2 V, which is the same as CV analysis. The specific capacitance was calculated from the galvanostatic discharge curves (Fig. 8) according to the following equation:

$$C_{sp} = \frac{I\Delta t}{\Delta V}$$

where C_{sp} is the specific capacitance (F g^{-1}), I is the current density (A g^{-1}), and ΔV is the voltage difference. As it can be shown in Fig. 8a, the charge-discharge curve is almost symmetrical and a specific capacitance of 202 F g^{-1} was achieved at a constant current density of 10 A g^{-1} . The curves present a small IR drop which proves a reasonable resistance of prepared electrode and can be an evidence of relatively fast ion transport at the interface between the active materials of prepared electrode and the electrolyte.⁷ The linear voltage-time dependence can be as an evidence of superior capacitive behavior of coiled CNT/Ni-NW based electrodes. It is noteworthy that the results of this method are in good agreement with the results were obtained from Cyclic voltammetry.

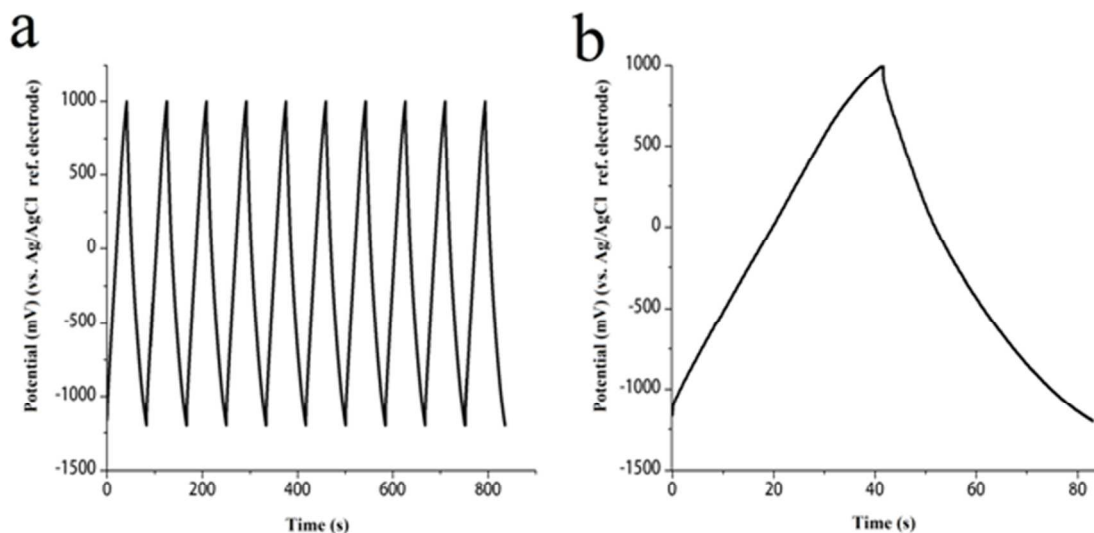


Fig. 8. (a) Galvanostatic charge/discharge curves of coiled CNTs electrode obtained at current density of 10A g^{-1} coiled CNTs/electrode, (b) charge-discharge curve of coiled CNTs/Ni-NWs electrode at a current density of 10A g^{-1} .

It is critical for supercapacitors to determine the rate capability and also the durability of prepared electrode, by investigation of the capability to maintain large capacitances under high charge-discharge current densities and also the ability to retain initial capacitance after a large number of charge-discharge cycles,^{43, 44} respectively. Fig. 9 shows the variation of the specific capacitance of the prepared electrode as a function of cycle number. It can be clearly seen that the specific capacitance still remains at 92% of the initial capacitance after 6000 cycles, indicating that coiled CNT/Ni-NW electrode show a good cycling stability as the supercapacitor electrodes. Fig. S4† shows the SEM images of Coiled CNT/Ni-NW electrode after 6000 cycles, which indicates the stability of coiled CNT/Ni-NWs as active material. The inset in Fig. 9 illustrates the cycling performance of the coiled CNT/Ni-NW electrodes at the current density increasing from 10 to 80A g^{-1} . As current density rises to 80A g^{-1} , the coiled CNT/NW electrode still retain 76% (155F g^{-1}) of the capacity achieved at 10A g^{-1} . This proves the

effective accessibility for electrolyte ions even at a higher speed, which can attributed to its unique porous structure.

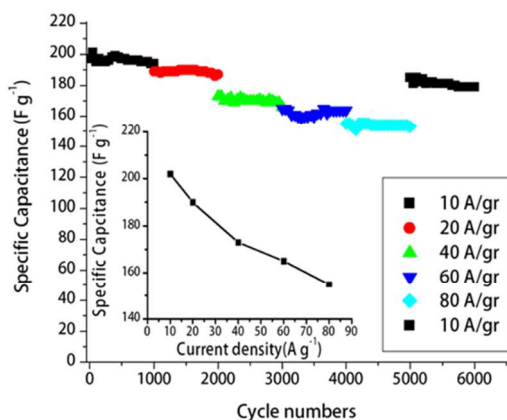


Fig. 9. Variation of the capacitance of coiled CNT electrode as a function of cycle number measured at different current densities from 10 to 80 A g⁻¹ and returning to 10 A g⁻¹, in 1.0 M Na₂SO₄ aqueous solution, inset: Specific capacitance measured at various charge/discharge current densities increasing from 10 to 80 A g⁻¹

Electrochemical impedance spectroscopy (EIS) is a suitable technique to evaluating the effect of the structure/distribution of active materials on current collectors on the capacitive performance of individual electrodes, and two-, multi electrode electrochemical devices.^{39, 43} EIS is a method which consisting of the application of the small perturbing current or voltage to an electrochemical system and measuring the response of the system. The response of the system can be described as impedance, Z , which is the ratio, or transfer function, of the voltage to the current. Because the perturbation is small, the response of the system is linear, and the same transfer function should result whether the applied signal is a potential difference or a current. Because some processes are related to the time derivations of potential and concentration rather than upon the magnitude of the variables themselves, some part of the system response will be

in-phase with the perturbation (a real component), and some part will be out-of-phase with the applied signal (an imaginary component).⁴⁵ The method is especially valuable because it also usually enables the equivalent series resistance (ESR) of the electrode structure and any potential dependent Faradic resistance.³⁹ Fig. 10 shows the Nyquist plot, which presents the results of EIS studies. As it is shown in Fig. 10, the theoretical Nyquist plot of a supercapacitor consists of three regions which are dependent on the frequency. At very high frequencies, which is remarked by A, supercapacitor behaves like a pure resistance.⁴⁶ The ESR is obtained from the real axis intercept of the Nyquist plot is 5.8 ohm for coiled CNT/Ni-NW electrode, which is composed of the electrolyte resistance, charge transfer resistance, and the contact resistance between the active material and the current collector.^{4, 39, 47} At low frequency region (part C), the plot being a nearly vertical line by sharply increasing of the imaginary part of impedance, which indicates a pristine capacitive behavior.^{46, 47} The influence of the porous structure and thickness of the electrode on the penetration of the electrolyte inside the electrode can be seen in the medium frequency range (part B).^{4, 43, 46, 47}

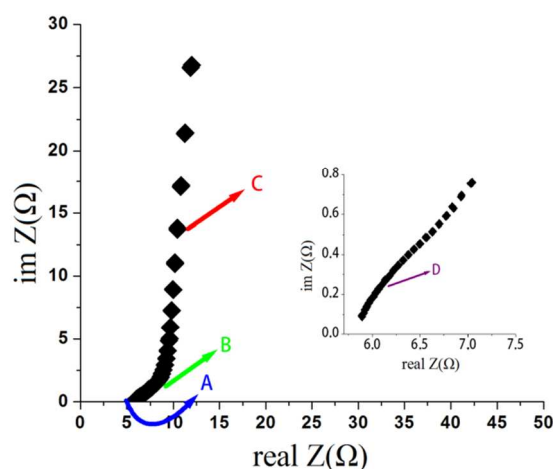


Fig. 10. Nyquist plots for coiled CNT/NW electrode in 1.0 M Na₂SO₄ aqueous solution, electrolyte over the frequency range of 100 kHz to 0.1 Hz.

In summary, we suggest that the excellent capacitive performance of the coiled CNT/Ni-NW electrode, which can be attributed to following factors: (1) high electric conductivity of coiled CNT/Ni-NW, resulted in high capacitance, especially at high scan rates (Fig. 10). (2) Porous structure of prepared electrode provides a large accessible surface area for charge storage which resulting in higher capacitance. (3) Fast electrode/electrolyte charge transfer which can attributed to binder-free electrodes.⁴⁸ Furthermore, combination of these excellent capacitive behavior with wide potential window making them as valuable candidate for improving supercapacitors with long cycle life.

4. Conclusions

We have successfully demonstrated a novel porous coiled CNT/Ni-NW nanostructure, by ambient thermal-CVD. This type of ductile CNT architecture, shows significantly enhanced supercapacitive performance, such as high stability (92% capacitance retention over 6000 cycles), high specific capacitance (202 F g^{-1} with a wide working potential window) which attributed to development of porous structure, excellent electron conductivity by existence of defects in coiled CNT structure, and good rate capability, as at high charge-discharge current densities, permeable porous structure of vertically aligned Ni-NWs contributed to the effective capacitive performance of coiled CNT/Ni-NW electrodes by facilitating the penetration of electrolyte ions at the electrode/electrolyte interface. Therefore, excellent electrochemical performance indicates that this material being a sufficient structure for improvement of electrode materials for advanced energy storage systems.

Electronic Supplementary Information: Fig. S1 shows the results of EDX analysis of the AAO after deposition of coiled CNTs by using catalytic chemical vapor deposition. The EDXs results prove the presence of CNTs and Ni nanowires on the AAO/Al based substrate.

Fig. S2 shows the XRD pattern of a coiled CNT/Ni-NW electrode before dissolving the AAO membrane. Fig. S3 shows CVs of the coiled CNT based electrode at different working potential windows at a scan rate of 100 mV s^{-1} in $1\text{M Na}_2\text{SO}_4$. Fig. S4 illustrates the SEM images of coiled CNTs and Ni-NWs after 6000 charge-discharge cycles.

References:

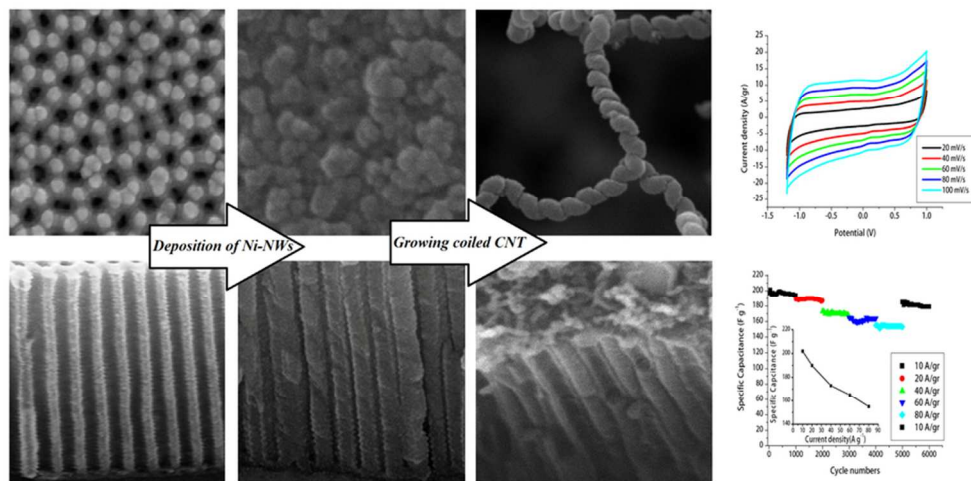
- (1) R. Kötz and M. Carlen, *Electrochim. Acta*, 2000, 45, 2483.
- (2) Y. Huang, J. Liang and Y. Chen, *Small*, 2012, 8, 1805.
- (3) P. Sharma and T. S. Bhatti, *Energ. Convers. Manage.*, 2010, 51, 2901.
- (4) J. Xu, Y. Dong, J. Cao, B. Guo, W. Wang and Z. Chen, *Electrochim. Acta*, 2013, 114, 76.
- (5) P. Simon and Y. Gogotsi, *Nat. Mater.*, 2008, 7, 845.
- (6) A. Lewandowski, A. Olejniczak, M. Galinski and I. Stepniak, *J. Power Sources*, 2010, 195, 5814.
- (7) W. Lu, L. Qu, K. Henry and L. Dai, *J. Power Sources*, 2009, 189, 1270.

- (8) W. Wang, S. Guo, M. Penchev, I. Ruiz, K. N. Bozhilov, D. Yan, M. Ozkan and C. S. Ozkan, *Nano Energy*, 2013, 2, 294.
- (9) F. Béguin, V. Presser, A. Balducci and E. Frackowiak, *Adv. Mater.*, 2014, 26, 2219.
- (10) W. Lu and L. Dai, in *Carbon Nanotubes*, ed. J. M. Marulanda, InTech, Vukovar, 2010, Ch. 29, pp. 563-589.
- (11) V. O. Khavrus, M. Weiser, M. Fritsch, R. Ummethala, M. G. Salvaggio, M. Schneider, M. Kusnezoff and A. Leonhardt, *Chem. Vapor Depos.*, 2012, 18, 53.
- (12) R. H. Baughman, A. A. Zakhidov and W. A. de Heer, *Science*, 2002, 297, 787.
- (13) S. Iijima, *Nature*, 1991, 345, 56.
- (14) M. Zhang and J. Li, *Mater. Today*, 2009, 12, 12.
- (15) X. B. Zhang, X. F. Zhang, D. Bernaerts, G. van Tendeloo, S. Amelinckx, J. van Landuyt, V. Ivanov, J. B. Nagy, Ph. Lambin and A. A. Lucas, *Europhys. Lett.*, 1994, 27, 141.
- (16) S. Motojima, I. Hasegawa, S. Kagiya, M. Momiyama, M. Kawaguchi and H. Iwanaga, *Appl. Phys. Lett.*, 1993, 62, 2322.
- (17) J. Prasek, J. Drbohlavova, J. Chomoucka, J. Hubalek, O. Jasek, V. Adam and R. Kizek, *J. Mater. Chem.*, 2011, 21, 15872.
- (18) J. A. Abu Qahouq and D. L. Carnaha, *Electron. Lett.*, 2012, 48, 639.
- (19) M. Kumar, in *Carbon Nanotubes - Synthesis, Characterization, Applications*, ed. S. Yellampalli, InTech, Vukovar, 2011, Ch. 8, pp. 147-170.

- (20) S. Amelinckx, X. B. Zhang, D. Bernaerts, X. F. Zhang, V. Ivanov and J. B. Nagy, *Science*, 1994, 265, 635.
- (21) H. Iwanaga, M. Kawaguchi and S. Motojima, *Jpn. J. Appl. Phys.*, 1993, 32, 105.
- (22) D. Pradhan and M. Sharon, *Mater. Sci. Eng. B*, 2002, 96, 24.
- (23) J. B. Bai, *Mater. Lett.*, 2003, 57, 2629.
- (24) S. Takenaka, M. Ishida, M. Serizawa, E. Tanabe, K. Otsuka, *J. Phys. Chem. B*, 2004, 108, 11464.
- (25) K. T. Lau, M. Lu and D. Hui, *Compos. Part B-Eng.*, 2006, 37, 437.
- (26) C. G. Jin, W. F. Liu, C. Jia, X. Q. Xiang, W. L. Cai, L. Z. Yao and X. G. Li, *J. Cryst. Growth*, 2003, 258, 337.
- (27) G. Meng, A. Cao, J. Y. Cheng, A. Vijayaraghavan, Y. J. Jung, M. Shima and P. M. Ajayan, *J. Appl. Phys.*, 2005, 97, 064303.
- (28) G. D. Sulka, A. Brzózka, L. Zaraska and M. Jaskuła, *Electrochim. Acta*, 2010, 55, 4368.
- (29) W. Hu, L. Yuan, Z. Chen, D. Gong and K. Saito, *J. Nanosci. Nanotechnol.*, 2002, 2, 203.
- (30) K. Nielsch, F. Müller, A. P. Li and U. Gösele, *Adv. Mater.*, 2000, 12, 582.
- (31) A. Cortés, G. Riveros, J. L. Palma, J. C. Denardin, R. E. Marotti, E. A. Dalchiele and H. Gómez, *J. Nanosci. Nanotechnol.*, 2009, 9, 1992.

- (32) J. H. Yen, I. C. Leu, M. T. Wu, C. C. Lin and M. H. Hon, *Electrochem. Solid St.*, 2004, 7, H29.
- (33) M. Chhowalla, K. B. K. Teo, C. Ducati, N. L. Rupasinghe, G. A. J. Amaratunga, A. C. Ferrari, D. Roy, J. Robertson and W. I. Milne, *J. Appl. Phys.* 2001, 90, 5308.
- (34) Z. Yang, X. Chen, H. Nie, K. Zhang, W. Li, B. Yi and L. Xu, *Nanotechnology* 2008, 19, 085606.
- (35) H. Kim, J. Kang, Y. Kim, B. H. Hong, J. Choi and S. Iijima, *J. Nanosci. Nanotechnol.*, 2011, 11, 470.
- (36) J. Wang, H. Chu and Y. Li, *ACS Nano* 2008, 2, 2540.
- (37) J. H. Yen, I. C. Leu, M. T. Wu, C. C. Lin and M. H. Hon, *Diam. Relat. Mater.*, 2005, 14, 841.
- (38) M. Liu and J. Sun, *J. Mater. Chem. A*, 2014, 2, 12068.
- (39) B. E. Conway, *Electrochemical Supercapacitors: Scientific Fundamentals and Technological Applications*, Plenum, New York, 1999.
- (40) L. Demarconnay, E. Raymundo-Piñero, F. Béguin, *Electrochem. Commun.* 2010, 12, 1275.
- (41) M. P. Bichat, E. Raymundo-Piñero, F. Béguin, *Carbon* 2010, 48, 4351.
- (42) Q. T. Qu, B. Wang, L. C. Yang, Y. Shi, S. Tian, Y. P. Wu, *Electrochem. Commun.* 2008, 10, 1652.
- (43) S. Wang and R. A. W. Dryfe, *J. Mater. Chem. A*, 2013, 1, 5279.

- (44) Y. Su and I. Zhitomirsky, *Colloid Surface A*, 2013, 436, 97.
- (45) J. P. Meyers, M. Doyle, R. M. Darling and J. Newman, *J. Electrochem. Soc.*, 2000, 147, 2930.
- (46) Q. Cheng, J. Tang, J. Ma, H. Zhang, N. Shinya and L. C. Qin, *Phys. Chem. Chem. Phys.*, 2011, 13, 17615.
- (47) P. L. Taberna, P. Simon and J. F. Fauvarque, *J. Electrochem. Soc.*, 2003, 150, A292.
- (48) H. F. Ju, W. L. Song and L. Z. Fan, *J. Mater. Chem. A*, 2014, DOI: 10.1039/C4TA00538D.



39x19mm (600 x 600 DPI)